**Supplemental Table 1. Characteristics of Preventive Cardiology Cohort, Related to Figure 1**

| Factor | Total (N=187) | No Diabetes (N=145) | Diabetes (N=42) | p-value* |
|---|---|---|---|---|
| Demographic | | | | |
| Age | 51.1±12.0 | 49.7 ±11.8 | 55.9±11.6 | 0.0034 |
| Male (%) | 98 (52.4) | 77 (53.1) | 21 (50.0) | 0.8578 |
| Current Smoker (%) | 45 (24.1) | 40 (27.6) | 5 (11.9) | 0.0590 |
| BMI | 29.4(26.4-35.1) | 28.7(25.8-33.9) | 32.8(28.4-38.1) | 0.00013 |
| Clinical | | | | |
| BPS | 126.0(117.2-137.0) | 123.5(114.8-136.2) | 130.0(122.0-141.8) | 0.0323 |
| BPD | 77.0(70.0-84.0) | 77.0(70.0-83.3) | 79(71.0-88.8) | 0.2880 |
| Cholesterol | 180.0(157.5-208.0) | 179.0(158.0-205.0) | 187.5(147.5-223.2) | 0.4258 |
| Triglycerides | 122.0(87.0-178.0) | 118.0(87.0-166.0) | 135.5(98.3-217.8) | 0.0624 |
| HDL | 43.0(35.5-51.5) | 44.0(36.0-54.0) | 41.0(35.5-47.8) | 0.2962 |
| LDL | 107.0(88.0-131.0) | 106.0(89.0-129.0) | 107.5(78.8-146.5) | 0.9445 |
| CRP | 1.8(0.5-5.5) | 1.6(0.5-4.9) | 2.3(0.9-7.6) | 0.1874 |
| HgbA1c | 5.2(4.9-6.0) | 5.1(4.7-5.5) | 6.25(5.9-7.7) | <0.0001 |
| Glucose/Insulin | 7.8(5.1-14.7) | 9.44(5.7-17.1) | 5.78(3.5-9.6) | 0.6402 |
| TMAO | 3.4(2.1-5.4) | 3.1(2.1-4.9) | 4.7(3.1-7.0) | 0.00086 |
| Choline | 8.0(6.6-9.8) | 7.9(6.6-9.7) | 8.3(6.6-10.0) | 0.5798 |
| Betaine | 41.1(30.6-51.6) | 44.6(33.5-53.2) | 31.8(26.8-41.8) | <0.0001 |

*p values were calculated by Wilcoxon-test for continuous data and Pearson's chi-square test for categorical factors.

**Supplemental Table 2. Characteristics of Hepatology Cohort, Related to Figure 1**

| Factor | Total (N=248) | No Diabetes (N=188) | Diabetes (N=60) | p-value* |
|---|---|---|---|---|
| Demographic | | | | |
| Age | 60.7±13.1 | 60.3 ±14.3 | 62.2±7.9 | 0.7676 |
| Male (%) | 132 (53.2) | 98 (52.1) | 34 (56.7) | 0.6420 |
| Current Smoker (%) | 17 (6.9) | 10 (5.3) | 7 (11.7) | 0.1613 |
| BMI | 29.2(25.5-32.3) | 28.0(25.1-31.4) | 31.2(28.4-34.9) | 0.00015 |
| Clinical | | | | |
| BPS | 122.0(112.0-130.0) | 120.0(112.0-130.0) | 122.0(114.8-130.0) | 0.5184 |
| BPD | 72.0(68.0-80.0) | 74.0(68.0-80.0) | 70(64.0-78.0) | 0.0024 |
| Cholesterol | 165.0(137.0-205.0) | 169.0(139.0-212.0) | 155.5(131.5-180.5) | 0.0298 |
| Triglycerides | 99.0(71.0-142.5) | 93.0(69.5-135.0) | 125.5(79.8-188.8) | 0.00075 |
| HDL | 47.0(39.0-55.0) | 49.0(41.0-57.5) | 41.5(34.8-47.3) | <0.0001 |
| LDL | 96.0(70.5-122.5) | 99.0(75.0-127.0) | 84.5(64.3-103.5) | 0.0084 |
| CRP | 1.4(0.6-3.45) | 1.3(0.5-2.70) | 2.2(1.15-7.4) | 0.00018 |
| HgbA1c | 5.4(5.1-5.8) | 5.3(5.0-5.6) | 6.3(5.6-6.9) | <0.0001 |
| Glucose/Insulin | 11.4(7.7-16.2) | 12.5(8.9-18.3) | 7.2(4.0-11.4) | 0.0022 |
| TMAO | 3.6(2.4-5.2) | 3.3(2.3-5.2) | 5.0(3.3-9.3) | <0.0001 |
| Choline | 6.9(5.7-8.4) | 6.7(5.6-8.1) | 8.0(6.3-9.5) | 0.00046 |
| Betaine | 38.3(29.0-49.8) | 38.9(29.7-49.5) | 35.6(27.4-51.7) | 0.3580 |

*p values were calculated by Wilcoxon-test for continuous data and Pearson's chi-square test for categorical factors.

**Supplemental Table 3. Characteristics of Combined Cardiology and Hepatology Cohorts, Related to Figure 1**

| Factor | Total (N=435) | No Diabetes (N=333) | Diabetes (N=102) | p-value* |
|---|---|---|---|---|
| Demographic | | | | |
| Age | 56.6±13.5 | 55.6 ±14.3 | 59.6±10.0 | 0.0142 |
| Male (%) | 230 (52.9) | 175 (52.6) | 55 (53.9) | 0.8974 |
| Current Smoker (%) | 62 (14.3) | 50 (15.0) | 12 (11.8) | 0.5094 |
| BMI | 29.3(25.8-33.2) | 28.4(25.4-32.4) | 31.6(28.4-36.3) | <0.0001 |
| Clinical | | | | |
| BPS | 122.0(114.0-133.0) | 122.0(113.0-132.0) | 126.0(117.2-134.5) | 0.0633 |
| BPD | 74.0(68.0-81.0) | 75.0(69.0-80.3) | 74(66.0-81.8) | 0.3627 |
| Cholesterol | 173.0(146.0-207.0) | 177.0(148.0-208.0) | 166.0(138.2-205.8) | 0.1089 |
| Triglycerides | 107.5(78.0-155.8) | 103.0(76.0-148.2) | 127.5(84.0-203.2) | 0.00025 |
| HDL | 45.5(37.0-55.0) | 46.0(38.0-56.0) | 41.0(35.0-47.8) | 0.00015 |
| LDL | 101.0(77.0-126.8) | 104.0(80.0-129.0) | 96.5(72.0-120.0) | 0.0246 |
| CRP | 1.6(0.6-4.4) | 1.4(0.5-3.8) | 2.3(1.0-7.4) | 0.00035 |
| HgbA1c | 5.3(5.0-5.9) | 5.2(4.9-5.5) | 6.3(5.7-7.1) | <0.0001 |
| Glucose/Insulin | 9.8(6.5-15.4) | 10.8(6.6-17.5) | 6.6(3.8-11.2) | 0.0127 |
| TMAO | 3.5(2.4-5.6) | 3.2(2.2-5.1) | 4.8(3.3-7.7) | <0.0001 |
| Choline | 7.5(6.1-9.1) | 7.3(6.0-8.7) | 8.1(6.4-9.6) | 0.0025 |
| Betaine | 39.3(29.9-51.1) | 41.0(30.3-51.7) | 33.8(27.2-45.1) | 0.00063 |

*p values were calculated by Wilcoxon-test for continuous data and Pearson's chi-square test for categorical factors.

**Supplemental Table 4**. **Dietary levels of free and lipid choline quantified by Liquid Chromotography-Tandem Mass Spectrometry, Related to Figure 3**

| | **Free Choline (mg/100mg diet)** | **Lipid Choline (mg/100 mg diet)** | **Total Choline (mg/100 mg/diet)** |
|---|---|---|---|
| **Chow** | 9.69 | 2.65 | 12.34 |
| **High Fat Diet** | 8.79 | 0.26 | 9.05 |

**Supplemental Table 5**. ***Fmo3*** **mutations identified in** ***Fmo3*** **mutant mice generated by the CRISPR/Cas9 technology**, **Related to Figure 5**

| **Identified *Fmo3* mutation*** | **Predicted mutation in FMO3 protein** |
|---|---|
| 1 bp insertion (A) at bp 89 of exon 2 | Frameshift, premature termination at a.a.-pos 74 |
| 7 bps deletion (bps 87-93) of exon 2 | Frameshift, premature termination at a.a.-pos 98 |
| 6 bps deletion (bps 88-93) of exon 2 | Two a.a. in-frame deletion (74-75 a.a.-pos) |
| 1 bp insertion (T) at bp 90 of exon 2 | Frameshift, premature termination at a.a.-pos 76 |
| 1 bp deletion (T) at bp 90 of exon 2 | Frameshift, premature termination at a.a.-pos 100 |

*: All mutations are located in the exon 2 of *Fmo3* gene, bp: base pair

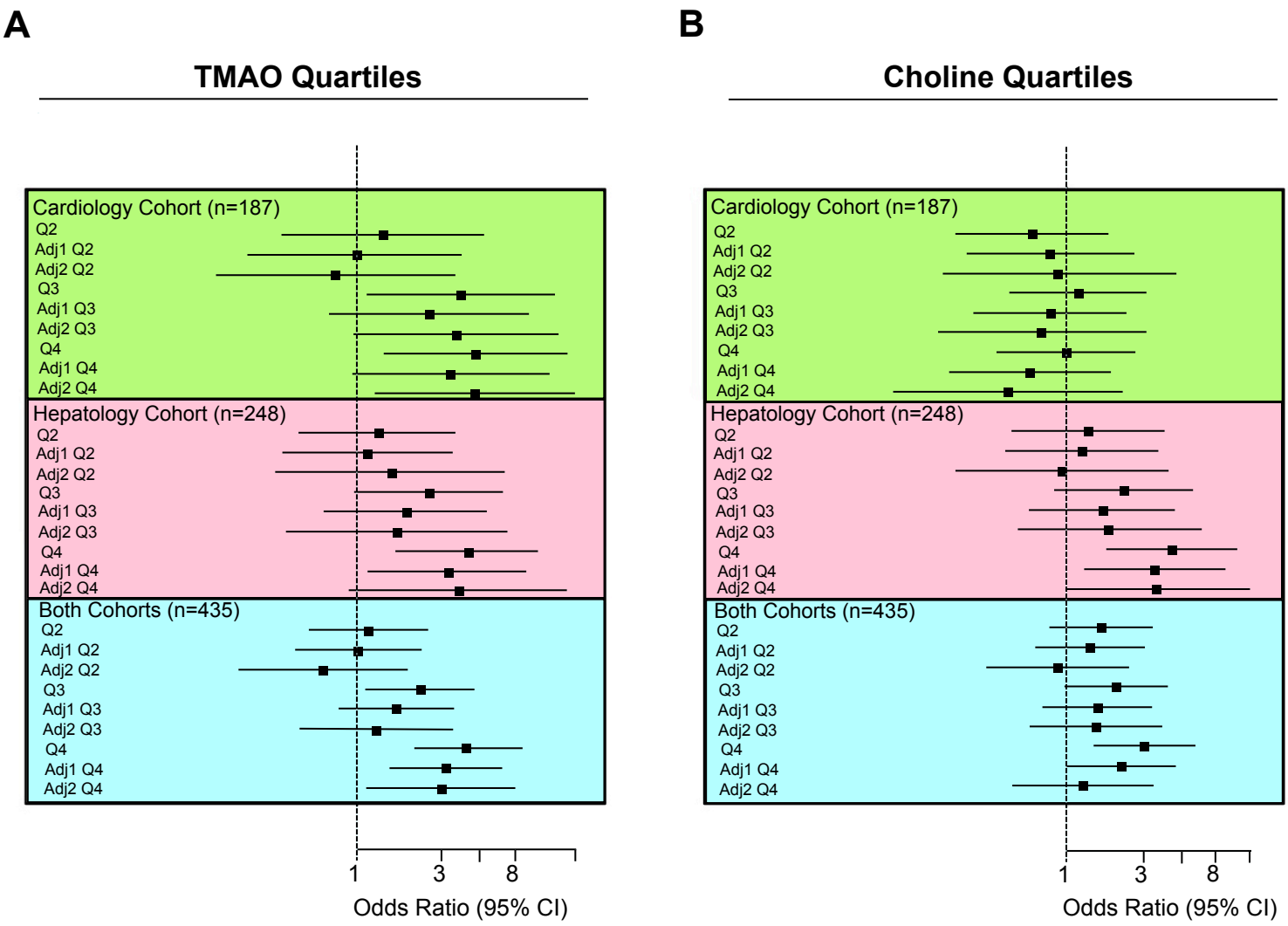


**Figure S1. After Adjustments for Multiple Comorbidities, Prevalent CVD and CVD Risk Factors, Medications, and Renal Function, TMAO Remains a Strong Predictor of T2DM Risk, Related to Figure 1.**

We recruited two separate cohorts of stable subjects in preventative cardiology (n=187) or hepatology clinics (n=248) to evaluate associations between fasting circulating TMAO or choline levels with prevalent type 2 diabetes (T2DM). The total number of subjects recruited in both studies was n=435. Patient demographics, laboratory values, and clinical characteristics are provided in detail in the Supplemental Table 1.

(A) Forest plots of the odds ratio of prevalent T2DM and quartiles of TMAO; bars represent 95% confidence intervals.

(B) Forest plots of the odds ratio of prevalent T2DM and quartiles of choline; bars represent 95% confidence intervals.

Adjusted Model 1 = Adj1: Adjusted for age, gender, current smoker, BMI, and systolic blood pressure.

Adjusted Model 2 = Adj2: Adjusted for age, gender, current smoker, BMI, and systolic blood pressure, glucose, triglycerides, HDL, and medication class.

Medication Classes Included: Analgesic-Aspirin, Analgesic-NSAID, Analgesic-Other, Cardiology-Antiarrhythmic, Cardiology-Anticoagulant, Cardiology-Other, Diabetes-Combo, Diabetes-Insulin, Diabetes-Other, Diabetes-Sulfonylurea, Diuretic-Fluid, Diuretic-Other, Food Suppl., GI-Antihistamine, GI-Other, HTN-A2 Receptors, HTN-Ace, HTN-Alpha 1, HTN-Beta Blocker, HTN-CCB, HTN-Central, HTN-Combination, HTN-Diuretic, HTN-Other, HTN-Peripheral, Infectious Antibiotic, Lipid Lower-Fibric Acid, Lipid Lower-Fish Oil, Lipid Lower-Niacin, Lipid Lower-Resin, Lipid Lower-Statin, Lipid Lower-Other, Mineral Suppl.-Other, Mineral Suppl.-Calcium, Mineral Suppl.-Iron, Nitrate, Psyche-Antidepressant, Psyche-Antianxiety, Psyche-Nontraditional, Psyche-Other, Respiratory-Steroid, Respiratory-Other, Steroid Hormones, and Vitamins.

**A**

**Validation Cohort #1: European American (n=99)**

| | Body Mass Index | | Fat % | | Insulin Sensitivity | | WAT *UCP1* Expression | |
|---|---|---|---|---|---|---|---|---|
| | r | *p* | r | *p* | r | *p* | r | *p* |
| ***FMO3* - v1** | 0.23 | 2.40*E*-02 | 0.23 | 2.30*E*-02 | -0.35 | 4.0*E*-04 | -0.22 | 3.17*E*-02 |
| ***FMO3* - v2** | 0.17 | 8.60*E*-02 | 0.17 | 1.00*E*-01 | -0.32 | 1.0*E*-03 | No Data | No Data |

**B**

**Validation Cohort #2: African American (n=256)**

| | Body Mass Index | | Matsuda Index | | Insulin Sensitivity | | WAT *PRDM16* Expression | |
|---|---|---|---|---|---|---|---|---|
| | r | *p* | r | *p* | r | *p* | r | *p* |
| ***FMO3* - v1** | 0.23 | 2.91*E*-04 | -0.16 | 1.0*E*-02 | -0.15 | 2.1*E*-02 | -0.27 | 1.6*E*-05 |
| ***FMO3* - v2** | 0.30 | 1.66*E*-06 | -0.20 | 2.0*E*-03 | -0.18 | 7.0*E*-03 | No Data | No Data |

**Figure S2. Validation Cohorts for Examining the Association Between Human White Adipose Tissue (WAT) *FMO3* Expression and Metabolic Traits, Related to Figure 2.**

To confirm findings in the large METSIM study, which only includes Finnish men, we examined the relationship between WAT *FMO3* expression and metabolic traits in two additional cohorts spanning both men and women of European American and African American ethnicity. The first cohort (panel A) included n=99 non-Hispanic Caucasian Americans, including 42 males and 57 females (Das et al., 2015). The second cohort (panel B) included n=260 African Americans, including 139 males and 121 females (Sharma et al., 2016). Data show the correlation between the two major *FMO3* transcript variants (v1, NM_001002294.1; v2, NM_006894.4) and metabolic traits. In addition, the correlation between WAT *FMO3* and markers of brown/beige adipocytes (*PRDM16* and *UCP1*) is shown.

(A) Correlation between human WAT *FMO3* mRNA expression and metabolic traits in European American men and women (n=99).

(B) Correlation between human WAT *FMO3* mRNA expression and metabolic traits in African American men and women (n=260).

Abbreviations: *PRDM16*, PR domain containing 16, *UCP1*, uncoupling protein 1.

## A Human Liver Biopsy Cohort Subject Characteristics

| | BMI <30 (n=10) | BMI ≥30 (n=40) | p value |
|---|---|---|---|
| **Age** | 50.90 ±4.30 | 46.35 ±2.00 | 0.3217 |
| **Female (%)** | 60.0 | 72.5 | - |
| **Weight (lbs)** | 157.74 ±8.03 | 235.99 ±17.00 | 0.0278 |
| **Insulin (μIU/ml)** | 6.78 ±2.75 | 9.41 ±1.58 | 0.4925 |
| **Fasting Glucose (mg/dl)** | 95.34 ±9.83 | 121.57 ±6.05 | 0.0508 |
| **HOMA-IR** | 2.03 ±1.03 | 3.36 ±0.84 | 0.4451 |
| **Plasma Cholesterol (mg/dl)** | 122.35 ±32.44 | 131.32 ±9.05 | 0.7112 |
| **Plasma Triglycerides (mg/dl)** | 172.84 ±10.37 | 169.90 ±7.23 | 0.8496 |
| **Liver Triglycerides (mg/g PR)** | 284.37 ±150.93 | 407.04 ±64.96 | 0.4174 |

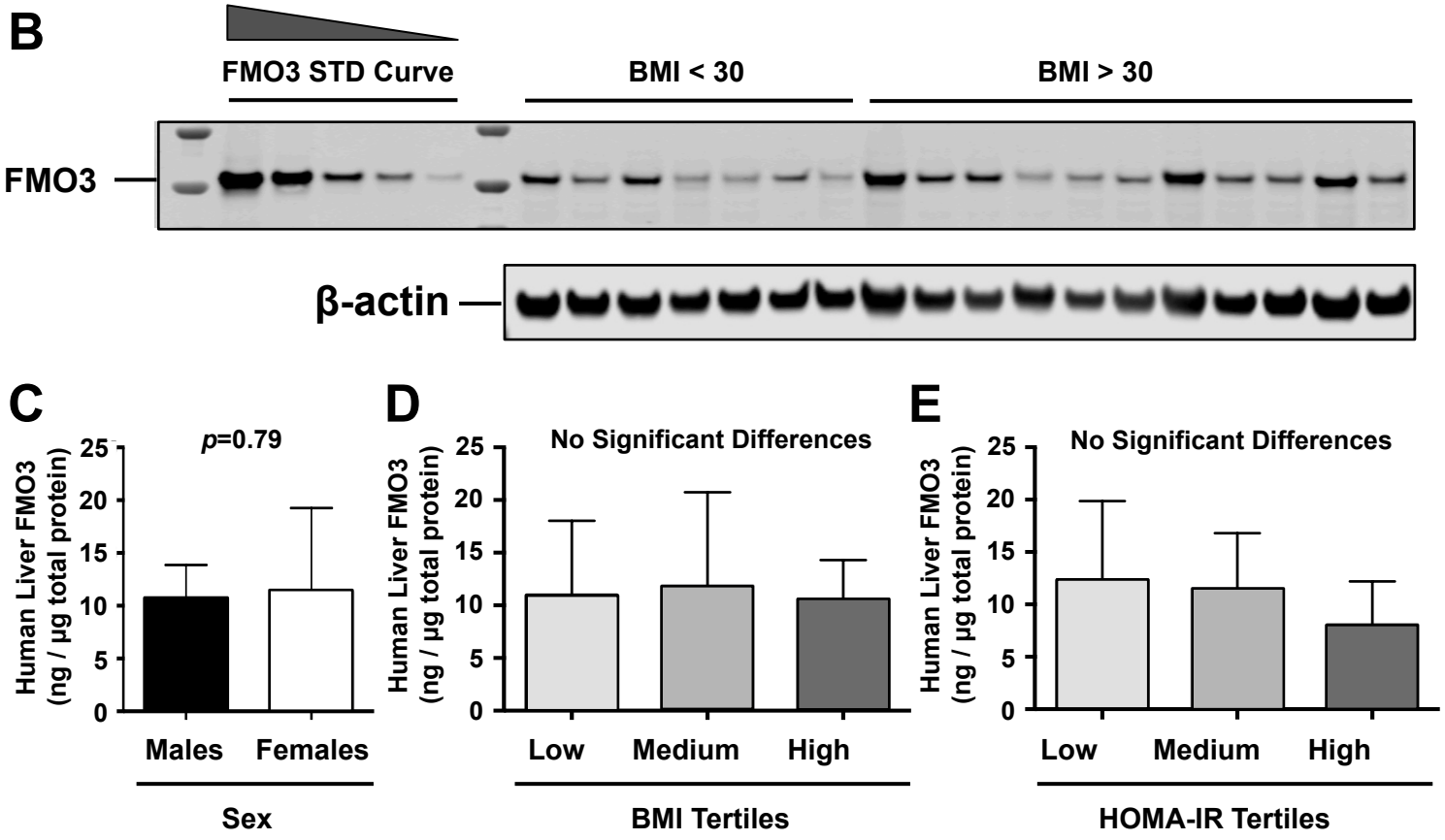


**Figure S3. FMO3 Protein Expression in Human Liver, Related to Figure 2.**

We recruited a cohort of surgical patients with a wide range of body mass index (BMI), and performed quantitative Western blotting to determine the abundance of FMO3 protein expression in relation to BMI. The total number of human livers assayed for FMO3 protein abundance was n=50.

(A) Patient demographics, laboratory values, and clinical characteristics separated by BMI.

(B) Representative Western blot showing a single band corresponding to the molecular weight of a recombinant hFMO3 protein standard curve.

(C) FMO3 protein abundance is not sexually dimorphic in human liver.

(D) FMO3 protein abundance is not different between low, medium, and high tertiles of BMI.

(E) FMO3 protein abundance is not different between low, medium, and high tertiles of Homeostatic Model Assessment of Insulin Resistance (HOMA-IR).

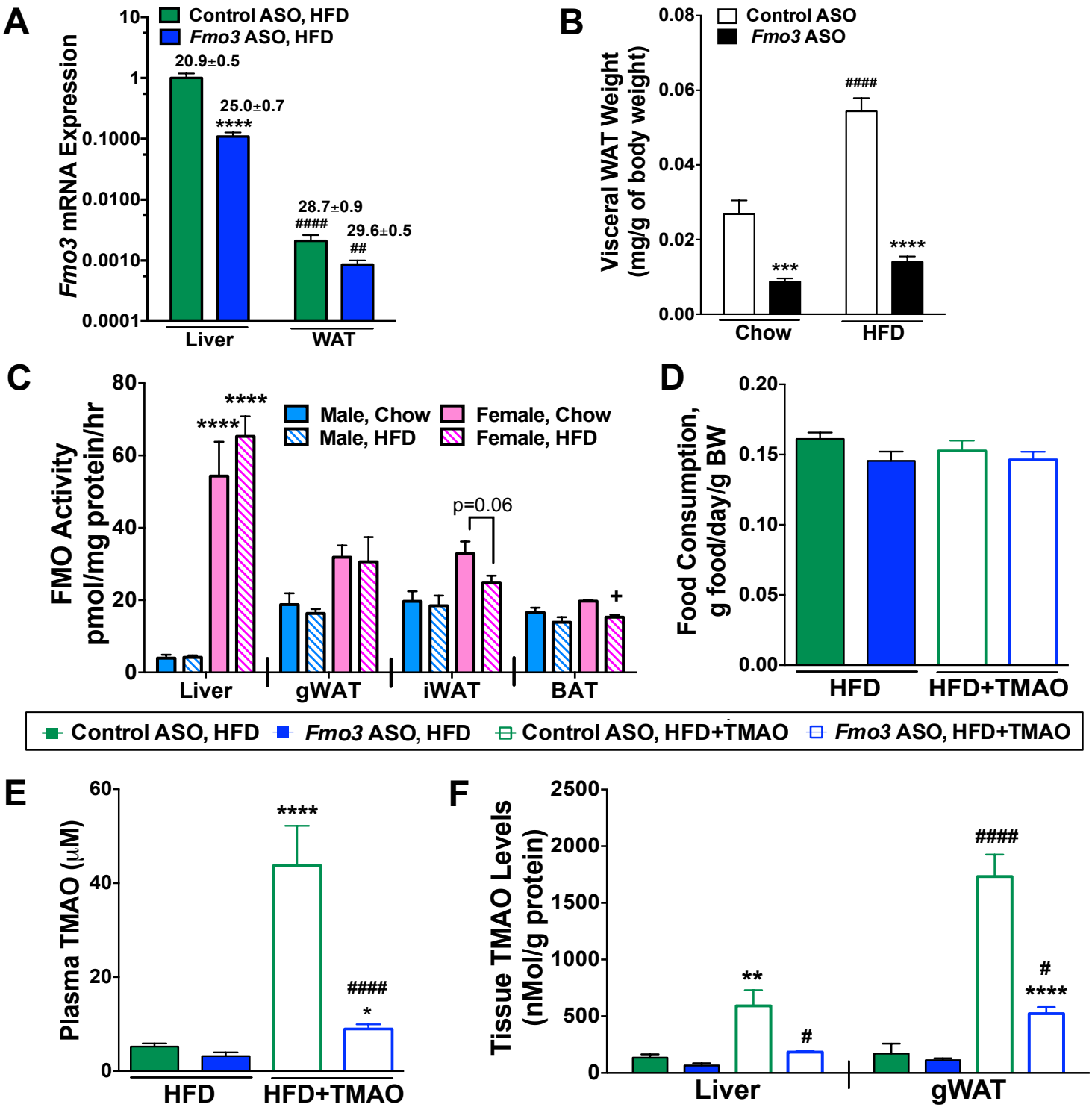


**Figure S4. Alterations in the TMA/FMO3/TMAO Pathway in Mouse Studies, Related to Figure 4.**

At 6-8 weeks of age, male and female C57BL/6 mice were treated with either a non-targeting control ASO or an ASO targeting knockdown of FMO3 in conjunction with either standard rodent chow or high fat diet (HFD) feeding as indicated.

(A) Relative *Fmo3* gene expression in matched liver and gonadal white adipose tissue samples of female mice fed HFD. Numerical values above bars indicate mean CT value detected by rtpcr, and gene expression is normalized to cyclophilin A in both tissues. ****, p≤0.0001 vs. same tissue in Control ASO-treated mice; ##, p≤0.01 and ###, p≤0.001 vs. ASO-matched liver samples two-way ANOVA.

(B) Gonadal white adipose tissue weight in male mice fed chow or HFD

(C) FMO enzymatic activity (d9-TMA to d9-TMAO conversion rates) in mouse tissues. ****, p≤0.0001 vs. male mice on same diet. +, p≤0.05 vs. female mice on chow

(D) Food consumption normalized to body weight in female mice maintained on HFD or HFD with 0.02% w/w TMAO (HFD+TMAO)

(E) Plasma and (F) Liver and gonadal white adipose tissue (gWAT) TMAO levels in female mice maintained on HFD or HFD+TMAO.*, p≤0.05, **, p≤0.01, ****, p≤0.0001 vs HFD, same tissue; #, p≤0.05 and ####, p≤0.0001 vs. Control ASO mice on same diet by two-way ANOVA

**Supplemental Experimental Procedures:**

**Human Studies:**

*Human Study # 1: Studies Examining Circulating Choline and TMAO Levels in Type 2 Diabetics (Related to Figure 1, Figure S1 and Supplemental Table 1).* To examine whether circulating choline and TMAO levels were associated with type 2 diabetes risk, we recruited two unique cohorts with diverse cardiometabolic risk profiles. Both studies we approved by the Cleveland Clinic Institutional Review Board, and every subject provided written informed consent. For the cardiology cohort, sequential subjects (n=187) presenting to the Preventive Cardiology Clinic at the Cleveland Clinic with suspicion of fatty liver were consented and enrolled for a registry. Fasting blood was collected into EDTA vacutainer tubes, maintained on ice, and processed into plasma, and frozen at -80$^{o}$C within 2 hours of collection. For the hepatology cohort, sequential subjects (n=248) presenting to the Hepatology Clinic at the Cleveland Clinic for planned diagnostic liver biopsy were consented and enrolled for a sample repository and clinical data registry. Fasting blood was collected into EDTA vacutainer tubes, maintained on ice, and processed into plasma, and frozen at -80$^{o}$C within 2 hours of collection. Type 2 diabetes diagnosis was classified according to the American Diabetes Association criteria (American Diabetes Association, Diagnosis and classification of diabetes mellitus. 2016, Diabetes Care 39, Suppl 1: S54-55). Plasma levels of TMAO were quantified using the quantitative LC/MS-MS method described below and as previously published (Wang et al., 2014). Given this is the first published description of these cohorts, we provide detailed tables above with patient demographics, laboratory values, and clinical characteristics.

Human Study # 2: *Large Population Adipose Tissue Microarray Cohort (Related to Figure 2E):* To examine the relationship between *FMO3* expression and metabolic traits, we took advantage of a large population-based study with subcutaneous adipose biopsy as an endpoint. The Metabolic Syndrome in Men (METSIM) study is a cross-sectional longitudinal study that included 10,197 men, aged from 45 to 73 years randomly selected from the population of Kuopio Finland and examined in 2005-2010 (http://www.nationalbiobanks.fi/index.php/studies2/10-metsim). The aim of the study was to investigate genetic and non-genetic factors associated with the risk of type 2 diabetes, cardiovascular disease, and insulin resistance–related traits in a cross-sectional and longitudinal setting. A detailed description of clinical characteristic, laboratory values, and metabolic phenotyping has been published previously (Stancakova et al., 2009; Stancakova et al., 2011). Glucose tolerance was classified according to the American Diabetes Association criteria (American Diabetes Association, Diagnosis and classification of diabetes mellitus. 2016, Diabetes Care 39, Suppl 1: S54-55). and the Matsuda Index was calculated as previously described (Matsuda and DeFronzo, 1999). The study was approved by the ethics committee of the University of Eastern Finland and Kuopio University Hospital and was conducted in accordance with the Helsinki Declaration. All study participants gave written informed consent. For the data shown in Figures 2E, subcutaneous fat biopsy samples were obtained from a random sample of the participants (n = 770) of the METSIM baseline study (age 54.8 ± 5.1 years; BMI 26.6 ± 3.5 kg/m$^2$). Total RNA was isolated from these samples using Qiagen miRNeasy Kit according to the manufacturer's instructions. RNA integrity number values were assessed with the Agilent Bioanalyzer 2100and samples with RNA integrity number >7.0 were used for transcriptional profiling. Expression profiling using Affymetrix U219 microarray was performed at the Department of Applied Genomics Bristol-Myers Squibb according to manufacturer's protocols. The probe sequences were reannotated to remove probes that mapped to multiple locations, contained SNPs with greater than 1% MAF as assessed in 1,000 genomes European populations in their target sequences, and did not map to known transcripts based on the RefSeq (version 59) and ENSEMBL (version 72) databases. For subsequent analysis we used 43,145 probesets that represent 18,155 unique genes. The microarray image data were processed using the Affymetrix GCOS algorithm, utilizing quantile normalization or the robust multiarray (RMA) method to determine the specific hybridizing signal for each gene. Expression data can be obtained from Gene Expression Omnibus (GEO) database with the accession number GSE70353.

Study # 3: *Validation Adipose Tissue Microarray Studies in Ethnically Diverse Cohorts (Related to Figure S2):* Given that the large population adipose tissue microarray study (METSIM) only included Finnish men, we set out to validate mRNA expression data in several distinct cohorts spanning both men and women of European American and African American ethnicity. Importantly, both of the selected validation cohorts had extensive insulin sensitivity data evaluated by Minimal model analysis (MINMOD) of frequently sampled intravenous glucose tolerance tests (FSIVGT). The first cohort included n=99 non-Hispanic Caucasian Americans including 42 males and 57 females. All participants provided written informed

consent under protocols approved by the University of Arkansas for Medical Sciences (IRB #53028) and by the Institutional Review Board at Wake Forest School of Medicine (IRB#00011083). A detailed description of clinical characteristics, laboratory values, and metabolic phenotyping has been published previously (Das et al., 2015). The second cohort included n=260 African Americans including 139 males and 121 females. All participants provided written informed consent under protocols approved by the Institutional Review Board at Wake Forest School of Medicine (IRB#00015775). A detailed description of clinical characteristic, laboratory values, and metabolic phenotyping of this unique population has been published previously (Sharma et al., 2016). Both of these populations underwent subcutaneous adipose biopsies, with subsequent microarray analysis using the Illumina HT12-V4 expression beadchip platform (Das et al., 2011; Das et al., 2015; Sharma et al., 2016), This Illumina platform included two expressed probes for *FMO3*: ILMN_2344283 (NM_001002294.1) and ILMN_1808657 (NM_006894.4). The expression of the two *FMO3* probes were strongly correlated (r>0.93, Pearson correlation coefficient), thus to evaluate the correlation of *FMO3* with other brown/beige adipocyte transcripts, we used only ILMN_2344283 (NM_001002294.1) for the comparison.

Study # 4: *Human Liver Biopsy Cohort (Related to Figure S3):* The purpose of this study was to examine the relationship between hepatic FMO3 expression and metabolic phenotypes such as steatosis, hyperlipidemia, insulin sensitivity, and obesity in humans. The majority of subjects recruited here were morbidly obese bariatric surgery patients, but we were able to obtain liver biopsies from 11 subjects with a BMI under 30 as normal weight controls. For recruitment, adult patients undergoing gastric bypass surgery at Wake Forest School of Medicine provided written consent and were enrolled by a member of the study staff following institutionally approved IRB protocols. Exclusion criteria included: positive anti-hepatitis C antibody, positive hepatitis B surface antigen, or circulating hepatitis B DNA, history of liver disease other than NAFLD, Childs A, B, or C cirrhosis, past or present diagnosis/treatment of malignancy other than non-melanomatous skin cancer, INR greater than 1.8 at baseline or need for chronic anticoagulation with warfarin or heparin products, use of immunomodulation for or history of inflammatory diseases including but not limited to malignancy, rheumatoid arthritis, psoriasis, lupus, sarcoidosis and inflammatory bowel disease, and greater or equal to 7 alcohol drinks per week or 3 alcoholic drinks in a given day each week. In addition to bariatric surgery patients, a small number of non-obese subjects (body mass index <30.0) consented to liver biopsy during elective gall bladder removal surgery (n=11). Each subject was assigned a unique identifier which was used throughout the study and did not include any identifiable information about the patient such as name, address, telephone number, social security number, medical record number or any of the identifiers outlined in the HIPAA Privacy Rule regulations. Only the principal investigator had access to the code linking the unique identifier to the study subject. Basic clinical information was obtained via self-reporting and a 15 ml baseline blood sample was obtained at the time of enrollment. A subset of this cohort has been previously described (Shores et al., 2011). At the time of surgery, a roughly 1 gram sample from the lateral left lobe was collected by the surgeon. Wedge biopsies were rinsed with saline and immediately snap frozen in liquid nitrogen in the operating room before subsequent storage at -80°C. For quantification of hepatic FMO3 protein levels, whole liver protein lysates were made in a modified RIPA buffer as previously described (Brown et al., 2004), and protein was quantified using the BCA assay (Pierce). In order to quantify absolute amounts of hepatic FMO3, a protein standard curve was created using recombinant FMO3 supersomes (Corning). Patient proteins along with recombinant protein standard curves were separated by 4–12% SDS-PAGE, transferred to polyvinylidene difluoride (PVDF) membranes, and proteins were detected after incubation with specific antibodies as previously described (Brown et al., 2004; Brown et al., 2008a; Brown et al., 2008b; Brown et al., 2010). Antibodies used for immunoblotting were anti-FMO3 rabbit polyclonal (ABCAM #Ab126790) and anti-β actin rabbit monoclonal (Cell Signaling Technologies #4970).

**Hybrid Mouse Diversity Panel (HMDP) Studies Examining the Link Between TMAO and Obesity Traits (Related to Figure 2A-2D)**

92 inbred strains of 8-week-old male mice (180 individual mice) were fed a high fat and high sucrose diet (D12266B, Research Diets, New Brunswick, NJ) for 8 weeks before tissue collection (Parks et al., 2013). Plasma TMAO levels were measured and correlated with obesity-related traits using biweight midcorrelation analysis.

**Mouse Studies Using Antisense Oligonucleotide (ASOs) to Knockdown the TMAO-Producing Enzyme FMO3 (Related to Figures 3 and 4)**

To study the role of the TMAO-producing enzyme FMO3 in diet-induced obesity and insulin resistance, we employed an in vivo knockdown approach in adult mice (6-8 weeks of age). Antisense oligonucleotide (ASO)-mediated knockdown was accomplished using 20-mer phosphorothioate ASOs designed to contain 2'-0-methoxyethyl groups at positions 1 to 5 and 15 to 20 as we have previously published (Warrier et al., 2015). All ASOs used in this work were synthesized, screened, and purified as described previously (Crooke et al., 2005) by Ionis Pharmaceuticals, Inc. (Carlsbad, CA). For FMO3 knockdown studies, young (6-8 week old) female C57BL/6 mice were purchased from Harlan (Indianopolis, IN, USA), and maintained on either a standard rodent chow diet or a high fat diet (45% of energy from Lard; Brown et al. 2010) and injected intraperitoneally biweekly with 25 mg/kg of either non-targeting control ASO (5'-TCCCATTTCAGGAGACCTGG-3') or an ASO directed against murine *Fmo3* (5'-TGGAAGCATTTGCCTTTAAA-3') for a period of 6-20 weeks, according to experimental endpoint. For magnetic resonance imaging studies (Figure 3F-3J), mice were treated with ASOs for a period of 14 weeks before imaging. For cold tolerance studies (Figure 4E), mice were treated with ASOs and maintained on a high fat diet for 5 weeks before being housed for 6 hours under room temperature (22$^{o}$C) or cold condition (4$^{o}$C) before necropsy under the same conditions. For indirect calorimetry studies (Figure 4F-4H), mice were treated with ASOs and fed a high fat diet for 16 weeks prior to study, and allowed to equilibrate to metabolic cage environments for ~ 48 hours before entering into 24 hour periods at thermoneutrality (30$^{o}$C), room temperature (22$^{o}$C), or cold temperature (4$^{o}$C). Oxygen consumption ($VO_2$), heat, and respiratory exchange ratio (RER) were constantly monitored using the Oxymax CLAMS home cage system (Columbus Instruments). For dietary TMAO addback studies (Figure 4I-4K), female C57BL/6 mice were injected intraperitoneally with either a control ASO or *Fmo3* ASO (50 mg/kg body weight per week) for a total of 12 weeks while being maintained on the high fat diet described above, or the same diet supplemented with TMAO (0.2%, wt/wt) as previously described (Warrier et al., 2015). For experiments examining the fasting/fed transition (Figure 6D-6H), mice were treated with ASOs for 6 weeks and all sacrificed between 7:00-8:00 am (beginning of light cycle), with the fasted group having had food removed 12 hours prior at 7:00 pm. analysis. For ASO studies, all mice were maintained in an Association for the Assessment and Accreditation of Laboratory Animal Care, International-approved animal facility, and all experimental protocols were approved by the institutional animal care and use committee of the Cleveland Clinic.

**Generation of FMO3 Knockout Mice Using Clustered Regularly Interspaced Short Palindromic Repeats with Cas9 Nuclease (CRISPR-Cas9) Technology (Related to Figure 5)**

The target sequence (5'-GATAGGGCTACTGAAAGGGT-3') complementary to a region in exon 2 of the coding sequence of mouse *Fmo3* was used for guide RNA construction. The Cas9 mRNA and guide RNA targeting *Fmo3* were microinjected into the fertilized mouse eggs of strain C57BL/6 to generate mice that potentially carry the *Fmo3* gene mutations. DNA samples from the potential *Fmo3* mutant mice were PCR-amplified using primers located in the intron 1 (AGAGTGCTGATTGCATATGGC) and intron 2 (AGTCTCGGGCCTCCTTATCA) region of mouse *Fmo3,* generating a 493 bp PCR product. The PCR product was subjected to denaturing and reannealing, followed by cleavage by the Surveyor DNA endonuclease (Integrated DNA technologies, Coralville, Iowa) that recognizes this single-strand loop within the DNA amplicon, introducing a double-strand break at that location. Therefore, DNA samples from homozygous (wild-type or in rare cases of exact same mutant on both alleles) mice will not be cleaved, whereas those from the heterozygous mice will be cleaved into 338 bp and 155 bp DNA fragments. Seven founder mice carrying mutations in the target region of *Fmo3* were identified using this method (data not shown). We subsequently sequenced cloned PCR products of the target region of those seven to determine the nature of those mutations. Five different small in/del mutations that result in frame-shift mutation and premature termination of FMO3 protein were identified (supplemental Table 2) and further characterized (Supplemental Table 2). All FMO3 knockout animal experiments were approved by the UCLA Animal Care and Use Committee in accordance with PHS guidelines. Eight month old female wild-type (*Fmo3*+/+), heterozygous ($Fmo3^{+/-}$), and homozygous ($Fmo3^{-/-}$) littermates were fed a chow diet supplemented with 1.3% choline chloride for 12 weeks before tissue collection. In a second study, $Fmo3^{-/-}$ mice were crossed onto the $Ldlr^{-/-}$ background to generate $Ldlr^{-/-};Fmo3^{-/-}$ and $Ldlr^{-/-};Fmo3^{+/+}$ littermates. Two-month-old female $Ldlr^{-/-};Fmo3^{-/-}$ and $Ldlr^{-/-};Fmo3^{+/+}$ mice were fed a Western diet (RD-D12079B, Research Diets, New Brunswick, NJ) for 12 weeks before tissue collection. Obesity related traits were collected as previously described (Shih et al., 2015).

**Measurement of Plasma Trimethylamine and Trimethylamine-N-oxide (Related to all Figures)**

Quantification of TMA and TMAO in human or mouse plasma was performed using stable isotope dilution HPLC with online electrospray ionization tandem mass spectrometry on an API 365 triple quadrupole mass spectrometer (Applied Biosystems, Foster, CA) with upgraded source (Ionics, Bolton, ON, Canada) interfaced with a Cohesive HPLC (Franklin, MA) equipped with phenyl column (4.6 × 250 mm, 5 μm Silica (2), Morton Grove, IL), and the separation was performed as reported previously (Wang et al., 2011; Wang et al., 2014). TMAO and TMA were monitored in positive MRM MS mode using characteristic precursor-product ion transitions: m/z 76 →58 and m/z 60→44, respectively. The internal standards TMAO-trimethyl-d9 (d9-TMAO) and TMA-d9 (d9-TMA) were added to plasma samples before sample processing and were similarly monitored in MRM mode at m/z 85→68 and m/z 69→49, respectively. Various concentrations of TMAO and TMA standards and a fixed amount of internal standards were spiked into control plasma to prepare the calibration curves for quantification of plasma TMAO and TMA. For d9-TMA and d9-TMAO quantification in FMO activity analyses, 1,1,2,2-d4 choline (Sigma) was used as an internal standard followed by a 0.5 ml 3K cutoff centrifugal filter (Millipore) of sample prior to LC/MS/MS analysis. The characteristic precursor-product ion transition for 1,1,2,2-d4 choline is m/z 108→60 monitored in positive MRM MS mode.

**Measurement of Total Tissue Flavin Monooxygenase (FMO) Activity (Related to Supplemental Figure 3)**

Determination of enzymatic activity of tissue FMOs was conducted in 250 μl reaction mix containing 1 mg tissue protein homogenate, 100 μM d9-TMA, and 100 μM reduced nicotinamide adeninedinucleotide phosphate (NADPH) in 10 mM HEPES (pH 7.4). Reaction was stopped 8 hr later with 0.2 N formic acid, followed by filtering through a 3 K cutoff spin filter, and then snap frozen and stored at −80°C until time of analysis. For analyses, internal standard was added to the thawed filtrate, which was then injected onto an HPLC column with online tandem mass spectrometer to measure the oxidized product d9-TMAO as described above. Control studies performed omitting NADPH did not show conversion of TMA into TMAO.

***In Vivo* Body Composition by MRI (Related to Figure 3F-3J)**

Relaxation-Compensated Fat Fraction (RCFF) MRI was used to provide quantitative in vivo assessments of subcutaneous and peritoneal adipose tissue volumes as well as lean body mass as previously described (Johnson et al., 2012). Briefly, each animal was anesthetized in 1-2% isoflurane and positioned in a 7T Bruker Biospec (Bruker Inc., Billerica, MA) MRI scanner. The respiration rate (60 +/- 20 breaths / minute) and core body temperature (35 +/- 1C) were controlled throughout the imaging experiment. The RCFF-MRI acquisition was then used to generate high-resolution coronal MRI images of the entire mouse at different echo times (Figure 3). All images were then exported for offline processing in Matlab (The Mathworks, Natick, MA). The RCFF-MRI image analysis method first generates separate fat and water images sets and then mathematically recombines these fat and water images to calculate fat fraction images [fat / (water + fat)] compensated for both T1 and T2 relaxation times. These quantitative fat fraction images provide the basis for automatic segmentation of adipose tissue (fat fraction > 0.8) from other tissues such as liver and muscle. Subsequent segmentation of the peritoneal wall calculates peritoneal and subcutaneous adipose tissue volumes as well as lean body mass for each animal using the adipose tissue volumes and the total body weight for each animal.

**Immunoblotting (Related to Figure 5)**

Immunoblotting experiments were performed as previously described (Shih et al., 2015). The primary antibodies against FMO3 and β-actin were purchased from Abcam, Inc. (Cambridge, MA) and Cell Signaling Technology (Danvers, MA), respectively

**Real-Time PCR Analysis of Gene Expression (Related to Figures 3A, 4B, 4E, 4J, 4K, 5H, 6F-6H)**

Tissue RNA extraction was performed as previously described for all mRNA analyses (Brown et al., 2008a; Brown et al., 2008b; Brown, et al., 2010; Lord et al., 2012). Quantitative real time PCR (qPCR) analyses were conducted as previously described (Brown et al., 2008a; Brown et al., 2008b; Brown, et al., 2010; Lord et al., 2011). mRNA expression levels were calculated based on the ΔΔ-CT method. qPCR was conducted using the Applied Biosystems 7500 Real-Time PCR System.

Primers used for qPCR are available on request.

**Histological Analysis (Related to Figure 4A)**

Hematoxylin and eosin staining of paraffin-embedded gonadal adipose sections was performed as previously described (Brown et al., 2010).

**Quantification of Adipose β1AR Density and cyclic AMP (cAMP) Levels (Related to Figure 4C, 4D)**

βAR density was determined by incubating 20 μg of the membranes (plasma membranes) with saturating concentrations of [$^{125}$I]-cyanopindolol (250 pmol/L) alone or along with 100 μM propranolol for non-specific binding as described previously (Naga Prasad et al., 2001; Vasudevan et al., 2011). Furthermore, to distinguish between β1AR and β2ARs, 20 μg of the membranes were pre-incubated with either 100 μM metoprolol (a selective β1AR blocker) or ICI 118,551 (a selective β2AR blocker) followed by saturating concentrations of [$^{125}$I]-cyanopindolol. After 1 hour of incubation at 37°C, the membranes were harvested onto filters and measured for receptor density as described previously (Naga Prasad et al., 2001). Adenylyl cyclase (AC) assays were carried out by incubating 20 μg of membranes (isolated plasma membranes or endosomes) at 37°C for 15 minutes with labeled α$^{[32]}$P-ATP as previously described (Choi et al., 1997; Nienaber et al., 2003). Isoproterenol was used instead of albuterol in the plasma membranes/endosomal resensitization experiments because Isoproterenol is a full agonist, which allows for higher G-protein coupling resulting in measurable levels of in vitro cAMP generation especially in the endosomal fractions. The cAMP content was determined in the cytosol using catch point cAMP kit (Molecular Devices; Sunnyvale, CA) as per manufacturer's instruction (Vesudevan et al., 2011).

**Statistical Analysis**

To examine the association between circulating choline and TMAO with type 2 diabetes Wilcoxon rank-sum tests were used for continuous variables and $\chi 2$ tests for categorical variables were used to examine the differences between participants who had diabetes events and those who did not. Logistic regression models were used to estimate odds ratio and 95% confidence interval for diabetes. All analyses were performed using R 3.1.0 (Vienna, Austria) and $p < 0.05$ was considered statistically significant. All mouse data were analyzed using either one-way or two-way analysis of variance (ANOVA) where appropriate, followed by Student's t tests for post hoc analysis. Differences were considered significant at $p < 0.05$. All mouse data analyses were performed using JMP Pro 10 (SAS Institute; Cary, NC) or Graphpad Prism 6 (La Jolla, CA) software.

**Supplemental References:**

Barbosa-Morais, N.L., Dunning, M.J., Samarajiwa, S.A., Darot, J.F., Ritchie, M.E., Lynch, A.G., and Tavare, S. (2010). A re-annotation pipeline for Illumina BeadArrays: improving the interpretation of gene expression data. Nucleic Acids Res. *38*, e17.

Brown, J.M., Boysen, M.S., Chung, S., Fabiyi, O., Morrison, R.F., and McIntosh, M.K. (2004). Conjugated linoleic acid induces human adipocyte delipidation: autocrine/paracrine regulation of MEK/ERK signaling by adipocytokines. J. Biol. Chem. *279*, 26735-26747.

Brown, J.M., Chung, S., Sawyer, J.K., Degirolamo, C., Alger, H.M., Nguyen, T., Zhu, X., Duong, M.N., Wibley, A.L., Shah, R., et al. (2008a). Inhibition of stearoyl-coenzyme A desaturase 1 dissociates insulin resistance and obesity from atherosclerosis. Circulation *118*, 1467-1475.

Brown, J.M., Bell, T.A. 3$^{rd}$, Alger, H.M., Sawyer, J.K., Smith, T.L., Kelley, K., Shah, R., Wilson, M.D., Davis, M.A., Lee, R.G., et al. (2008b). Targeted depletion of hepatic ACAT2-driven cholesterol esterification reveals a non-biliary route for fecal sterol loss. J. Biol. Chem. *16*, 10522-10534.

Brown, J.M. Betters, J.L., Lord, C., Ma, Y., Han, X., Yang, K., Alger, H.M., Melchior, J., Sawyer, J.K., Shah, R., et al. (2010). CGI-58 knockdown in mice causes hepatic steatosis but prevents diet-induced obesity and glucose intolerance. J. Lipid Res. *51*, 3306-3316.

Choi, D.J., Koch, W.J., Hunter, J.J., and Rockman, H.A. (1997). Mechanism of beta-adrenergic receptor desensitization in cardiac hypertrophy is increased beta-adrenergic receptor kinase. J. Biol. Chem. *272*, 17223-17229.

Crooke, R.M., Graham, M.J., Lemonidis, K.M., Whipple, C.P., Koo, S., and Perera, R.J. (2005). An apolipoprotein B antisense oligonucleotide lowers LDL cholesterol in hyperlipidemic mice without causing hepatic steatosis. J. Lipid Res. *46*, 872-884.

Das, S.K., Sharma, N.K., Hasstedt, S.J., Mondal, A.K., Ma, L., Langberg, K.A., Elbein, S.C. (2011). An integrative genomics approach identifies activation of thioredoxin / thioredoxin reductase-1-mediated oxidative stress defense pathway and inhibition of angiogenesis in obese nondiabetic human subjects. J Clin Endocrinol Metab. *96*, E1308-1313.

Izem, L., and Morton, R.E. (2009). Molecular cloning of hamster lipid transfer inhibitor protein (apolipoprotein F) and regulation of its expression by hyperlipidemia. J. Lipid Res. *50*, 676-684.

Johnson, D.H., Narayan, S., Wilson, D.L., Flask, C.A. (2012). Body composition analysis of obesity and hepatic steatosis in mice by relaxation compensated fat fraction (RCFF) MRI. J. Magn. Reson. Imaging *35*, 837-843.

Lord, C.C., Betters, J.L., Ivanova, P.T., Milne, S.B., Myers, D.S., Madenspacher, J, Thomas, G., Chung, S., Liu, M., Davis, M.A. et al. (2012). CGI-58/ABHD5-derived signaling lipids regulate systemic inflammation and insulin action. Diabetes *61*, 355-363.

Naga Prasad, S.V., Barak, L.S., Rapacciuolo, A., Caron, M.G., and Rockman, H.A. (2001). Agonist-dependent recruitment of phosphoinositide 3-kinase to the membrane by beta-adrenergic receptor kinase 1. A role in receptor sequestration. J. Biol. Chem. *276*, 18953-18959.

Nienaber, J.J., Tachibana, H., Naga Prasad, S.V., Esposito, G., Wu, D., Mao, L., and Rockman, H.A. (2003). Inhibition of receptor-localized PI3K preserves cardiac beta-adrenergic receptor function and ameliorates pressure overload heart failure. J. Clin. Invest. *112*, 1067-1079.

Shi, W., Oshlak, A., and Smyth, G.K. (2010). Optimizing the noise versus bias trade-off for Illumina whole genome expression BeadChips. Nucleic Acids Res. *38*, e204.

Shores, N.J., Link, K., Fernandez, A., Geisinger, K.R., Davis, M.D., Nguyen, T., Sawyer, J., and Rudel, L.L. (2011). Non-contrasted computed tomography for the accurate measurement of liver steatosis in obese patients. Dig. Dis. Sci. *56*, 2145-2151.

Stancakova, A., Civelek, M., Saleem, N.K., Soininen, P., Kangas, A.J., Cederberg, H., Paananen, J., Pihlajamaki, J., Bonnycastle, L.L., Morken, M.A., et al. (2012). Hyperglycemia and a common variant of GCKR are associated with the levels of eight amino acids in 9,369 Finnish men. Diabetes *6*, 1895-1902.

Vasudevan, N.T., Mohan, M.L., Gupta, M.K., Hussain, A.K., and Naga Prasad, S.V. (2011). Inhibition of protein phosphatase 2A activity by PI3Kgamma regulates beta-adrenergic receptor function. Mol. Cell *41*, 636-648.

Wang, Z., Levison, B.S., Hazen, J.E., Donahue, L., Li, X.M., and Hazen, S.L. (2014). Measurement of trimethylamine-N-oxide by stable isotope dilution liquid chromatography tandem mass spectrometry. Anal. Biochem. *15*, 35-40.